The Structure of DNA within Cationic Lipid/DNA Complexes

Chad S. Braun,* Gouri S. Jas,[†] Sirirat Choosakoonkriang,* Gary S. Koe,[‡] Janet G. Smith,[‡] and C. Russell Middaugh*

*Department of Pharmaceutical Chemistry, University of Kansas, Lawrence, Kansas 66047; [†]Higuchi Bioscience Center, University of Kansas, Lawrence Kansas 66047; and [‡]Valentis Inc., Burlingame, California 94010

ABSTRACT   The structure of DNA within CLDCs used for gene delivery is controversial. Previous studies using CD have been interpreted to indicate that the DNA is converted from normal B to C form in complexes. This investigation reexamines this interpretation using CD of model complexes, FTIR as well as Raman spectroscopy and molecular dynamics simulations to address this issue. CD spectra of supercoiled plasmid DNA undergo a significant loss of rotational strength in the signal near 275 nm upon interaction with either the cationic lipid dimethyldioctadecylammonium bromide or 1,2-dioleoyltrimethylammonium propane. This loss of rotational strength is shown, however, by both FTIR and Raman spectroscopy to occur within the parameters of the B-type conformation. Contributions of absorption flattening and differential scattering to the CD spectra of complexes are unable to account for the observed spectra. Model studies of the CD of complexes prepared from synthetic oligonucleotides of varying length suggest that significant reductions in rotational strength can occur within short stretches of DNA. Furthermore, some alteration in the hydrogen bonding of bases within CLDCs is indicated in the FTIR and Raman spectroscopy results. In addition, alterations in base stacking interactions as well as hydrogen bonding are suggested by molecular dynamics simulations. A global interpretation of all of the data suggests the DNA component of CLDCs remains in a variant B form in which base/base interactions are perturbed.

INTRODUCTION

It is well established that complexes of cationic lipids and plasmid DNA (CLDCs) can deliver genes to cells both in vitro and in vivo. Despite the success of this approach, which has reached the stage of extensive human clinical trials, the relationship between the structure of such complexes and their ability to produce appropriate gene expression remains relatively undefined. In fact, the structure of the DNA itself within CLDCs is still a matter of controversy. CLDC long-range structure has been characterized with small-angle x-ray scattering and cryoelectron microscopy (Koltover et al., 1998; Xu et al., 1999; Radler et al., 1998). These analyses suggest that mesophases are formed in which DNA is enclosed by lipid bilayers in either lamellar or inverted hexagonal phases that are stacked to form higher order structures. The state of the DNA within these mesophases is not, however, clearly defined.

Recently, spectroscopic characterization of CLDCs using Raman, FTIR, UV/visible, fluorescence, and CD spectroscopies has been used to evaluate the structure of the individual components (Deng et al., 2000; Choosakoonkriang et al., 2001a,b; Braun et al., 2001). Vibrational spectroscopy suggests that the DNA maintains a B form conformation and

is dehydrated at the lipid interface (Hirsch-Lerner and Barenholz, 1999; Choosakoonkriang et al., 2001a). This work also reveals, as expected, that primary lipid/DNA interactions occur between the negatively charged phosphates of the DNA backbone and the positively charged lipid headgoups. Changes in lipid methylene vibrations also indicate that the apolar region of the lipid bilayer becomes further fluidized when DNA is bound (Davies et al., 1990; Choosakoonkriang et al., 2001a; Mendelsohn et al., 1989, 1991). These techniques are limited, however, by a lack of sensitivity, requiring formation of complexes at high concentrations, a condition under which colloidal stability is compromised. CLDCs form lyotropic mesophases that are known to have a strong dependence on concentration, making extrapolation to lower, more biologically and clinically relevant conditions difficult (Kabanov et al., 1998). In contrast, CD spectroscopy can be used to measure the long-range structure of DNA directly at concentrations from 10- to 100-fold lower than those used in vibrational spectroscopy. CD is particularly sensitive to the precise nature of the helical state of the DNA. The weak chirality of lipids allows the signals from the DNA in CLDCs to be clearly resolved with little or no interference from the lipid component. Initial CD studies of cationic lipid/DNA systems have been interpreted to indicate that DNA assumes a C form conformation in direct contradiction to the FTIR results (Patil and Rhodes, 2000; Simberg et al., 2001; Akao et al., 1996; Zuidam et al., 1999; Choosakoonkriang et al., 2001a).

The size and complexity of CLDCs have the potential to introduce significant artifacts into their CD spectra. In general, the particles formed upon complexation are typically greater than ∼120 nm diameter and display a heterogeneous size distribution. These large sizes and the heterogeneous nature of the complexes including a concentrated and uneven

Abbreviations used: CLDC, cationic lipid/DNA complexes; CD, circular dichroism; FTIR, Fourier transform infrared; DDAB, dimethyldioctadecylammonium bromide; PSI, polymer and salt induced; DOTAP, 1,2-dioleoyltrimethylammonium propane; OD, optical density; ODN, oligonucleotide.

distribution of chromophores could give rise to significant absorption flattening effects (Wallace and Teeters, 1987; Mao and Wallace, 1984; Rodger and Ismail, 2000; Maestre and Reich, 1980; Glaeser and Jap, 1985). Furthermore, differential light scattering can occur when the particle dimensions are greater than one-quarter the wavelength of the incident light (Bustamante et al., 1983; Keller and Bustamante, 1986a,b) and the refractive indices for left and right circularly polarized light differ. In this work, we consider the role or lack thereof of such contributions to the CD spectra of CLDCs. After analysis of these effects, we examine the basis of the altered CD spectra of the DNA within CLDCs in terms of complementary FTIR and Raman analyses, model complexes, and finally molecular dynamics simulations. The effects of lipids in both the gel and liquid crystalline state as well as modification of these properties by incorporation of nonbilayer forming (helper) lipids (Hafez et al., 2001; Koltover et al., 1998) are also addressed. We find that the evidence for C form DNA in the complexes unconvincing, but rather that irregular changes in base/base interactions offer a better explanation for the observed spectra.

EXPERIMENTAL SECTION

Materials

Purified plasmids (>95% supercoiled) pMB 113 (9.2 kbp), pMB 237 (9.1 kbp), and pMB 290 (5.2 kbp) were provided by Valentis. The three plasmids were compared, and it was determined that each was in native B form and that their CD spectra did not differ significantly from one another (not illustrated). DDAB, DOTAP, 1,2-dioleoyl-*sn*-glycero-3-phosphatidyletha-nolamine, and cholesterol were purchased from Avanti Polar Lipids (Alabaster, AL). Poly(dG) · poly(dC) (4 kbp), poly(dA) · poly(dT) (~229 bp), poly(dGdC) · poly(dGdC) (724 bp), and poly(dAdT) · poly(dAdT) (3.2 kbp) ODNs were acquired from Amersham Pharmacia Biotech (Piscataway, NJ). Purified single-stranded ODNs (20 bases) of poly(dA), poly(dT), poly(dC), poly(dG), poly(dAdT), and poly(dCdG) were synthesized by Operon Technologies (Alameda, CA). All polynucleotides were judged to be better than 98% pure as determined by mass spectrometry.

Preparation of CLDC

Liposomes were prepared by drying a lipid containing chloroform solution in a glass vial with a stream of nitrogen. The thin film formed was dried for a minimum of 2.5 h under vacuum desiccation. The film was hydrated with 10 mM Tris buffer at pH 7.4 for 30 min at a temperature above the phase transition temperature of the highest T_c component lipid. Uniform single lamellar liposomes were formed by extrusion 10 times through a 100-nm pore size polycarbonate filter (Whatman, Clifton, NJ). Plasmids and duplex ODNs were prepared by diluting a stock solution to ~100–200 μg/ml. The concentrations of these solutions were determined using the UV absorbance at 260 nm (A_{260}) and a molar absorptivity coefficient of 6490 L × mole^{-1} × cm^{-1}. The concentration of single-stranded ODNs was obtained from the UV absorbance using the ssDNA molar absorptivity coefficients provided by Operon. Duplexes were formed by annealing at 5°C below the transition temperature (provided by Operon) of the corresponding double-stranded polynucleotide and cooling at ~0.5°C/min.

Liposomes were stepwise diluted to concentrations appropriate for equal volume mixing with DNA at each charge ratio. Complexation was conducted by rapid addition with 30–60 s of mixing in small volumes of 0.4–1.2 ml. The order of addition was selected to avoid passing through charge neutrality. All charge ratios indicated in the text are given as the ratio of positive to negative charge. Note, however, that molar and charge ratios are essentially equivalent in these systems.

METHODS

Circular dichroism

CD was performed with a model J-720 spectropolarimeter (Jasco, Easton, MD). Spectra were acquired in a 1-mm path length quartz cuvette at 20°C, the temperature maintained with a Peltier device. Spectra were measured as the average of three scans from 190 to 350 nm at a scan rate of 20 nm/min and buffer subtracted. Accurate determinations of peak position (± 0.3 nm) required some smoothing of data using Savitsky-Golay and Fast Fourier Transform algorithms with smoothed data compared to raw spectra to confirm a good fit. Data analysis was performed with Excel 2000 (Microsoft, Redmond, WA) for arithmetic and conversion functions whereas Origin 6.0 (Microcal Software, North Hampton, MA) was used for smoothing and plotting. Optical density (OD) spectra were acquired in conjunction with the CD spectra by converting a second channel high tension voltage output to OD using a Jasco algorithm.

FTIR spectroscopy

FTIR spectra were obtained with a Magna-IR 560 spectrometer (Nicolet, Madison, WI) equipped with a mercury-cadmium-telluride detector using an attenuated total reflectance method in which the sample solution was placed directly in a ZnSe trough element of effective pathlength 12 μm (Thermal A.R.K., SpectraTech, Shelton, CT). Spectra were obtained under dry air purge by coaddition of 256 interferograms. The interferograms were apodized using the Happ-Genzel function, with no zero filling, to give a final resolution of 4 cm^{-1}. The association band of water at 2200 cm^{-1} was used as a reference for subtraction of water. Baseline corrections (1804−904 cm^{-1}) and seven-point Satvisky-Golay smoothing were applied to the spectra. Peak positions were assigned by an algorithm in Omnic software (Nicolet).

Raman spectroscopy

Raman spectra were acquired with a Raman 2000 instrument (Chromex, Albuquerque, NM). Samples were excited at 785 nm with ~180 mW of power measured at the source. Raman scattering was collected by a thermoelectrically cooled charge-coupled-device of 1024 × 256 pixels. The frequency axis was calibrated with 4-acetamidophenol before acquiring sample spectra. Samples were measured at room temperature in a quartz cuvette as the accumulated average of 18 exposures of 100 s at a DNA concentration of 2–3 mg/ml. Baseline subtraction and data analysis was performed with Grams 32 software (Galactic Industries, Salem, NH).

Molecular dynamics simulation

Molecular dynamics simulation of DNA liposome interactions was performed with the force field and the potential parameters from the latest versions of CHARMM (all hydrogen) for nucleic acids (Foloppe and MacKerell, 1998; Foloppe and MacKerell, 1999) and lipids (Schlenkrich et al., 1996). The initial configuration of the system was constructed in several stages. A lipid monolayer was generated by placing 64 protonated 1,2-dimyristoyl-*sn*-glycero-3-phosphocholine (DMPC) molecules on an 8 × 8 grid. Random chain conformations were selected from a library distributed with CHARMM version 26. The positions of the lipids were optimized first by rigid-body translations and rotations of whole molecules and then by energy minimization of the system periodic boundary conditions in the

monolayer (xy) plane. The size of the square cell in the xy plane was kept fixed at 74 Å, leading to an area of 85.6 Å^2 per lipid, which was found to be optimal for simulations (Feller and Pastor, 1999). To maintain planarity, harmonic constraints of the form $k(z-z_0)^2$ were placed on the nitrogen atoms of DMPC, $k = 25$ kcal $\times$ mole^{-1} $\times$ Å^{-1} and $z_0 = 0$, to maintain average planarity of the monolayer. The B-DNA decamer of sequence C-T-C-T-C-G-A-G-A-G coordinates were taken from 196D.pdb (Goodsell et al., 1995). Initially, the DNA was placed 10.0 Å above the monolayer, oriented along the x axis. To search for optimal DNA:liposome interactions, we performed a systematic search in which the position of the DNA center of geometry was moved relative to the lipid center by -4, 0, and 4 Å along the x and y; and rotations by 0, 60, and 120° around x; -30, -15, 0, 15, and 30° around y; and 0, 30, 60, and 90° around z were applied. At each of the 540 starting points, a 20-ps molecular dynamics simulation was performed, using Langevin dynamics with a friction coefficient of 50 ps^{-1}, a bath temperature of 300 K, and a time step of 2 fs. This was followed by 5000 steps of geometry optimization using the Adopted Basis Newton-Raphson algorithm. A nonbonded cutoff of 12 Å was employed. Screening of electrostatic interactions was introduced by using a dielectric constant equal to $1/R$, with R being the interatomic distance (Brooks et al., 1983). Calculations for a typical grid point took 0.5 h on an SGI Origin 2400 supercomputer. The optimized structures were sorted by energy and lowest energy structures analyzed graphically using WaveLab ViewerPro.

Dynamic light scattering

Particle sizing was performed with a Brookhaven (Holtsville, NY) instrument and 9000AT autocorrelator configured with a 50-mW HeNe laser operating at 532 nm (JDS Uniphase) and an EMI 9863 photomultplier tube (PMT) mounted on a BI-200M goniometer. Measurements were taken at a 90° angle from the incident light. The autocorrelation function was analyzed using the method of cumulants (Koppel, 1972), and the resultant mean translation diffusion coefficients were converted to mean hydrodynamic radii by the Stokes-Einstein equation. Each sample was measured three times with the mean and standard deviation reported.

RESULTS

CD of CLDCs

The CD spectra of three different plasmids (pMB 113, pMB 237, and pMB 290) were found to be identical within experimental error and exhibited characteristic B form (10.4 bp/turn) spectra (not illustrated) (Tinoco et al., 1980; Johnson, 1994, 1996). The CD of plasmid DNA is significantly perturbed when complexed with two commonly employed cationic liposomes, DOTAP and DDAB. Examples of spectra at various charge ratios of DDAB or DOTAP in complexes with DNA are shown in Fig. 1, *A* and *B*. The characteristic features of the canonical B form, a positive band at 275 nm, negative signal at 245 nm, and crossover point near 258 nm, (Johnson, 1994; Ivanov et al., 1973) are altered. Changes include red shifting of both bands and a significant reduction in intensity of the 275-nm peak. The presence of the cationic lipids also appears to induce some degree of differential light scattering at charge ratios near or greater than neutrality as indicated by the presence of spectral "tails". This signal at extended wavelengths outside of absorbance bands is characteristic of the dispersive part of differential light scattering (Keller and Bustamante, 1986a). Spectra that appear flattened, at charge ratios between 1.25
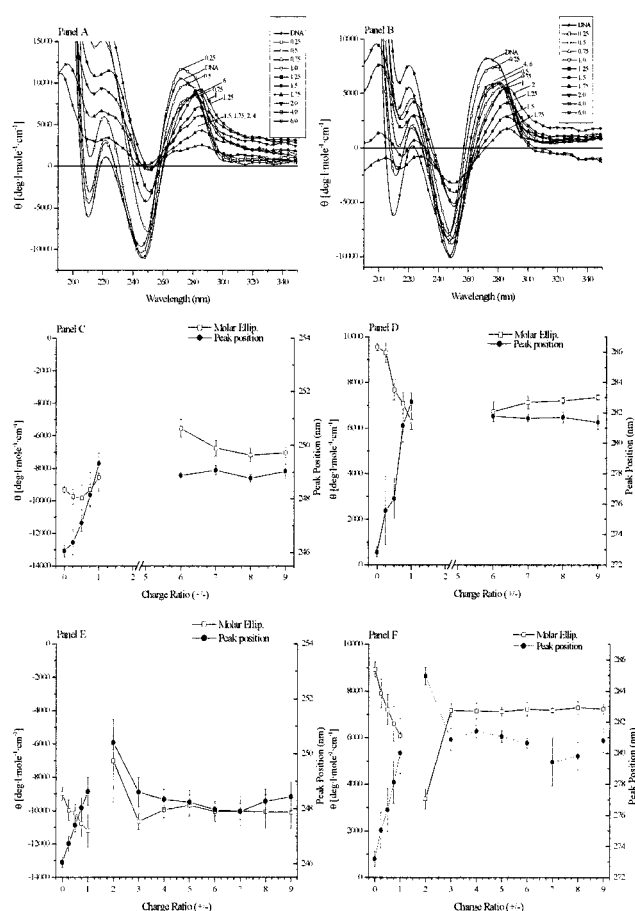

FIGURE 1 Representative CD spectra of DDAB/DNA (*A*) and DOTAP/DNA (*B*) complexes. The charge ratio is indicated on the spectra and in the legend. Open symbols are CLDCs below charge neutrality and closed symbols CLDCs above charge neutrality. Complexes were prepared with 50 μg/ml DNA in 10 mM Tris buffer, pH 7.4. The effect of lipid/DNA charge ratio (+/−) on CD spectra of DDAB/DNA (*C* and *D*) and DOTAP/DNA (*E* and *F*) complexes. The molar ellipiticity [deg $\times$ l $\times$ mole^{-1} $\times$ cm^{-1}] (*left axis*) and the peak position (*right axis*) are plotted versus charge ratio. The molar ellipiticity values are represented by open squares, whereas closed circles represent peak positions. Three titrations for each lipid were performed with a DNA concentration of 50–100 μg/ml. The 245-nm negative trough (*C* and *E*) and 275-nm peak (*D* and *F*) are plotted separately for each lipid.

and 4 with DDAB and 1.25–1.75 for DOTAP complexes, formed visible precipitates and were excluded from further analysis.

The molar ellipiticity and peak positions of the 245- and 275-nm bands are displayed as a function of charge ratio for DDAB and DOTAP lipoplexes in Fig. 1, *C–F*. The data in these plots have been normalized for concentration-dependent, dispersive light scattering by adjusting the baseline to zero based on an average value from 310 to 350 nm. The intensity changes generally reach their maximal values near charge neutrality. In the case of DDAB complexes at 245 nm, however, a small maxima in intensity occurs at a 0.5 charge ratio. As the fraction of DDAB is further increased, the 245-nm band is reduced to ~75% of the uncomplexed plasmid. The observed red shifts correlate with the intensity

changes in that the peak position shifts of both bands are greatest near a 1:1 lipid to DNA molar ratio. In CLDCs of DDAB, the peak positions shift up 3.3 and 8.6 nm for the 245 and 275 nm bands, respectively. When DOTAP is employed, the largest shifts were 2.6 nm for the 245-nm band and 7.6 nm for the 275-nm peak. The lack of spectral changes at high charge ratios suggests the formation of stable structures, but their final values remain significantly different from that seen in unliganded DNA.

Potential contributions of absorption flattening and differential scattering to CD spectra of CLDCs

In an attempt to unambiguously assign these altered spectra to a specific DNA conformation(s), we investigated the potential contribution of the two most common CD spectral artifacts. Because absorption flattening is a purely absorptive phenomenon, it can be investigated independently of CD contributions (Mao and Wallace, 1984). OD spectra of various DOTAP CLDCs show only small shifts in absorption maxima ($\leq$0.4 nm) in contrast to the 3- and 8-nm shifts seen in the CD bands (not illustrated). Furthermore, examination of CD spectra over a range of pathlengths and CLDC concentrations reveals little difference in concentration normalized data (data not shown). Both of these results are inconsistent with major contributions of absorption flattening to the CLDC CD spectra.

Differential scattering can distort CD spectra by anisotropically scattering light away from PMT detector. By moving the sample close to the detector, however, a collection angle of $>70°$ can be achieved. This can partially correct for dispersive light scattering by catching much of the differentially scattered light (Rodger and Ismail, 2000). In Fig. 2, the CD spectra of a 1:1 complex of DDAB and DNA show how spectra differ at various distances between the sample and PMT. As expected, the spectrum of the plasmid itself is unaffected by its distance from the PMT. The CLDC spectra, however, do show some distance dependence with the displacement of the spectrum from baseline larger at greater distances. It therefore appears that a greater collection angle ($72°$) is sufficient to correct for the majority of the differential scattering, but that this has little effect on the large decreases seen in the DNA peak at 275 nm in the CLDCs. Thus, differential scattering appears unable to account for the majority of the CLDC-induced spectral changes.

FTIR and Raman spectroscopy

Vibrational spectroscopy provides a complementary technique with which to examine the form of the DNA helix within lipoplexes. Although CD primarily monitors the interaction between adjacent nucleotides (i.e., coupled base/base interactions), both FTIR and Raman spectroscopy pri-
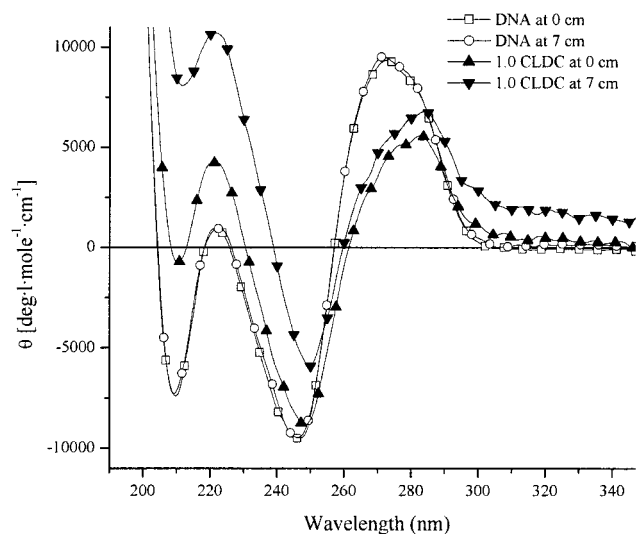
FIGURE 2   Representative CD spectra of plasmid DNA and DDAB/DNA complexes at a 1:1 charge ratio from samples placed at varying distance from the spectropolarimeter's detector. The spectrum of DNA itself (162 μg/ml) from samples placed 0.5 cm from the PMT is indicated by the open squares, and located 7 cm away by the open circles. The spectrum of a 1:1 charge ratio DDAB/DNA sample at the same concentration of DNA proximate to the detector is shown by the closed triangles and the more distant by the closed inverted triangles.

marily reflect local effects at the atomic level (Taillandier and Liquier, 1992; Thomas and Peticolas, 1983a,b; Nishimura and Tsuboi, 1986). Spectra from both methods (which differ in their selection rules) are shown in Fig. 3 and Fig. 4 at lipid/DNA charge ratios that exhibit maximal perturbation in their complementary CD spectra. It should be noted, that the vibrational methods require concentrations that are 10–20$\times$ the CD measurements. We find, however, that the size and ζ-potential of the complexes (as measured by dynamic and phase analysis light scattering, respectively) do not change over this concentration range. Furthermore, CD analysis conducted at FTIR and Raman concentrations using short pathlength cells produce spectra very similar to those seen at the lower concentrations (not illustrated). Several conformationally sensitive vibrations are present in the FTIR and Raman spectra of all lipid/DNA complexes. The most informative FTIR vibrations are the guanine/thymine carbonyl stretch (1715 cm^{-1}), thymine aromatic amine stretch (1328 cm^{-1}), symmetric and asymmetric phosphate stretches (1090 and 1223 cm^{-1}, respectively), and a strongly coupled sugar-phosphodiester signal (970 cm^{-1}) (Pichler et al., 1999; Colthup et al., 1975). The 1715, 1328, 1223, 1090, and 970 cm^{-1} bands are traditionally taken as markers of the B form and upon complexation their positions remain consistent with the presence of this form. This suggests that the conformation of the DNA in CLDCs remains in the B form. The helix-sensitive Raman signals include the symmetric phosphate stretch (1095 cm^{-1}), asymmetric phosphodiester (835 cm^{-1}), pyrimidine ring (785 cm^{-1}), guanine ring breathing (683 cm^{-1}), thymine aromatic amine stretch
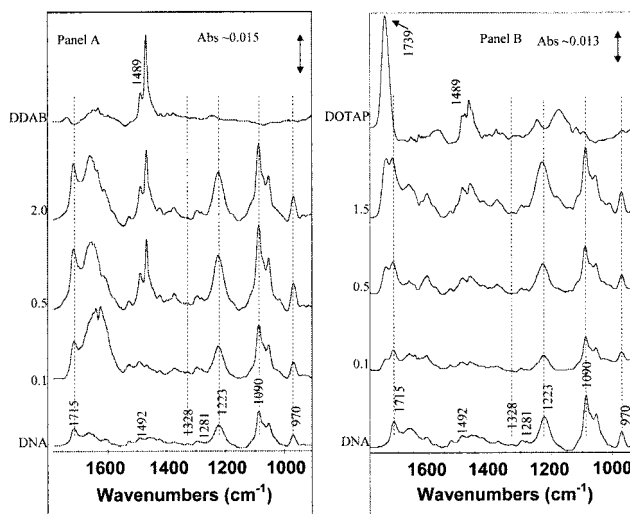
FIGURE 3 Representative FTIR spectra of DDAB/DNA (*A*) and DOTAP/DNA (*B*) complexes. The charge ratio is indicated to the left of each panel adjacent to the spectra. Peak positions are shown only on the spectra of the pure components. The vertical dotted lines are shown to facilitate the visualization of small peak shifts. Complexes were prepared with 2 mg/ml of DNA in 10 mM Tris buffer, pH 7.4.

(1375 cm^{-1}), and guanine N7 stretch (1489 cm^{-1}) modes (Serban et al., 2002). The regions from 600 to 700 cm^{-1} and 800 to 900 cm^{-1} are uniquely sensitive to the base-sugar conformation. In particular, B and C conformations are easily discerned by the position of the phosphodiester band, which at 875 cm^{-1} is indicative of C form, and when at 835 cm^{-1}, as in the unliganded plasmid, demonstrative of B form (Erfurth et al., 1972; Nishimura and Tsuboi, 1986; Peticolas et al., 1987). In both complexes, this region gives rise to additional peaks at 823 and 850 cm^{-1}. Due to their greater intensity than the 785 cm^{-1} band and splitting analogous to the 1095 cm^{-1} phosphate stretching, we believe these additional peaks reflect lipid/DNA interactions rather than a new nucleotide geometry. The 683 cm^{-1} peak of guanine is shifted to lower frequency ($\sim$5 cm^{-1}) in both CLDCs. The shifted DDAB and DOTAP CLDC peaks at 681 and 676 cm^{-1}, respectively, however, remain indicative of the C2′ endo-anti nucleotide conformation (Peticolas et al., 1987). Furthermore, the 1375 cm^{-1} thymine bands remain at 1374 cm^{-1} upon complexation, suggesting the C2′ endo-anti conformation (Nishimura and Tsuboi, 1986). This C2′-endo sugar pucker and anti sugar-base bond angle are the established nucleotide geometry of B form. There are three additional base vibrations altered in complexes, including adenine N6 amine (1422 cm^{-1}), guanine ring N7 (1488 cm^{-1}), and adenine/guanine ring N3 signals (1578 cm^{-1}) (Peticolas and Evertsz, 1992; Peticolas et al., 1987; Serban et al., 2002). These three prominent peaks in the plasmid are reduced or absent in the spectra of both complexes. A new peak also appears in the CLDC spectra at 1465 cm^{-1}, which can be assigned to the guanine ring N7 vibration in the hydrogen bonded state (Peticolas et al., 1987).
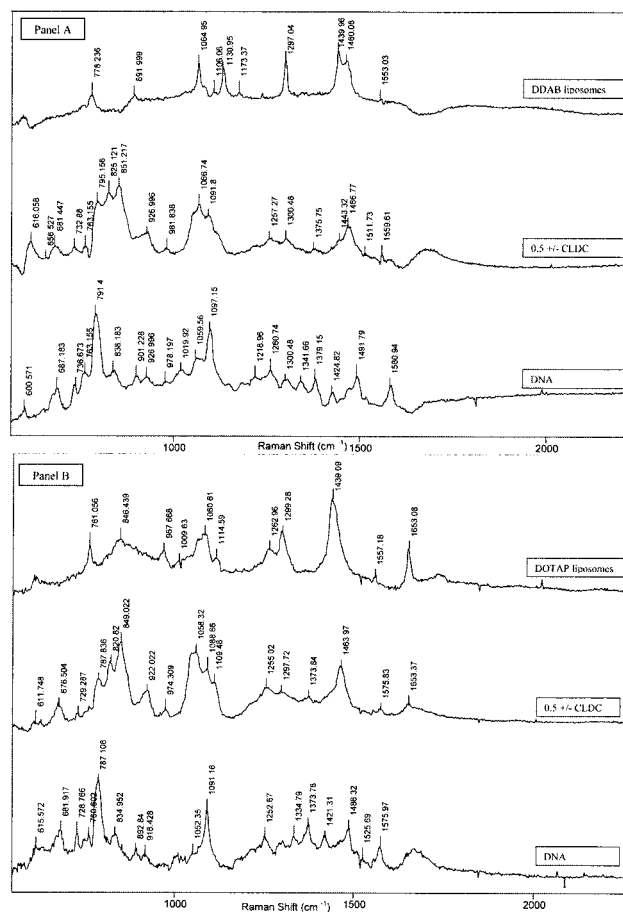

FIGURE 4 Representative Raman spectra of DDAB/DNA (*A*) and DOTAP/DNA (*B*) complexes at 0.5 charge ratio. The charge ratio is indicated to the right of the spectra. Complexes were prepared with 3 mg/ml of DNA in 10 mM Tris buffer, pH 7.4. The peak positions are labeled above the peak as the Raman shift in cm^{-1}.

Model studies

At this point we are faced with a conundrum. CD results suggest the DNA in CLDCs is in the C form whereas vibrational spectroscopic results are most consistent with the presence of B form. Absorption flattening cannot account for the spectral changes observed, whereas differential scattering, although present, appears minor and is also therefore an unlikely explanation. An alternative hypothesis is that lipid and DNA components in lamellar or inverted hexagonal arrangements further stack into a helical or some other higher order structure of opposite chirality to that of the ligated DNA. These signals would then be subtracted from the normal DNA peaks, reducing their intensity as observed. To address this hypothesis, the influence of basepair length on the CD induced by cationic lipid complexation was investigated with the idea that reducing ODN size should significantly alter the ability of the DNA to form chiral supramolecular structures. For this purpose, titrations of DOTAP into solutions of ODNs of differing lengths were conducted and CD spectra measured. Overall, the results suggest that small linear

dsDNA molecules produce spectra with changes similar to the much larger supercoiled plasmids. As an example, in Fig. 5 *A*, the titration of 20 bp poly(dG) · poly(dC) is shown because it exhibits the largest intensity and peak position changes of the model ODNs examined. As summarized in Table 1, all of the ODNs undergo significant intensity changes in both their long and short wavelength signals with addition of DOTAP. These spectral changes do not appear to correlate with basepair length. For example, the degree of change in intensity of poly(dG) · poly(dC) shows a 52% increase in 240-nm band intensity for the 4-kbp ODN, whereas at the same charge ratio (1.0), the much smaller 20-bp version manifests a similar 54% increase. Conversely, basepair length appears important in poly(dAdT) · poly(dAdT) and poly (dGdC) · poly(dGdC) where PSI-type (polymer and salt induced) spectra are observed for the 20-bp size but not the longer versions. PSI

type spectra are the result of differential light scattering within large particles containing DNA in a highly condensed state (Keller and Bustamante, 1986a,b). The poly(dGdC) · poly (dGdC) titration in Fig. 5 *B* produces spectra representative of this state at charge ratios from 3 to 5. The PSI-like effects are opposite to those seen in the plasmid spectra inasmuch as they involve large increases in peak intensity.

Molecular modeling of cationic liposome-DNA interactions

A molecular dynamics simulation was carried out to monitor the presence, if any, of dsDNA structural changes due to interaction between DNA and a cationic form of lipid monolayer of DMPC. A dsDNA (CTCTCGAGAG) containing 10 bp was brought near the stationary monolayer to model the interaction. DMPC was used because potential parameters for this lipid were readily available with the latest version of CHARMM nucleic acids and lipids. Although it is normally zwitterionic and therefore neutral, by protonating the phosphate group the surface contains positive charge alone and therefore can serve as a model of a cationic lipid. The dsDNA was allowed to move on the lipid surface using Langevin dynamics with a friction coefficient of 50 ps^{-1} to mimic water collisions. The dsDNA center of geometry relative to the lipid center was optimized until minimum interaction energies were obtained. Some resulting structures of the DNA at various stages of the minimization process are shown (Fig. 6) with the lipid removed for clarity. The dotted lines, which appear to terminate in space, represent hydrogen bonding between the DMPC headgroup and the bases. A striking alteration of the local helicity is immediately evident with base stacking interactions strongly perturbed, although the overall helicity of the duplex is still evident.

Effect of helper lipids on the CD of CLDCs

Because certain neutral lipids are routinely used to enhance transfection efficiency, two common neutral "helper" lipids, 1,2-dioleoyl-*sn*-glycero-3-phosphatidylethanolamine and cholesterol, were incorporated into the cationic lipid complexes (Huang et al., 1999) and their effect on the CD of CLDCs examined. Helper lipids were incorporated at a 1:1 molar ratio to the cationic host lipid, a ratio at which they are known to enhance transfection efficiency (Felgner et al., 1994). Addition of helper lipids to CLDCs results in minor CD spectral differences from the spectra of equivalent charge ratio complexes composed solely of the cationic lipid (data not shown).
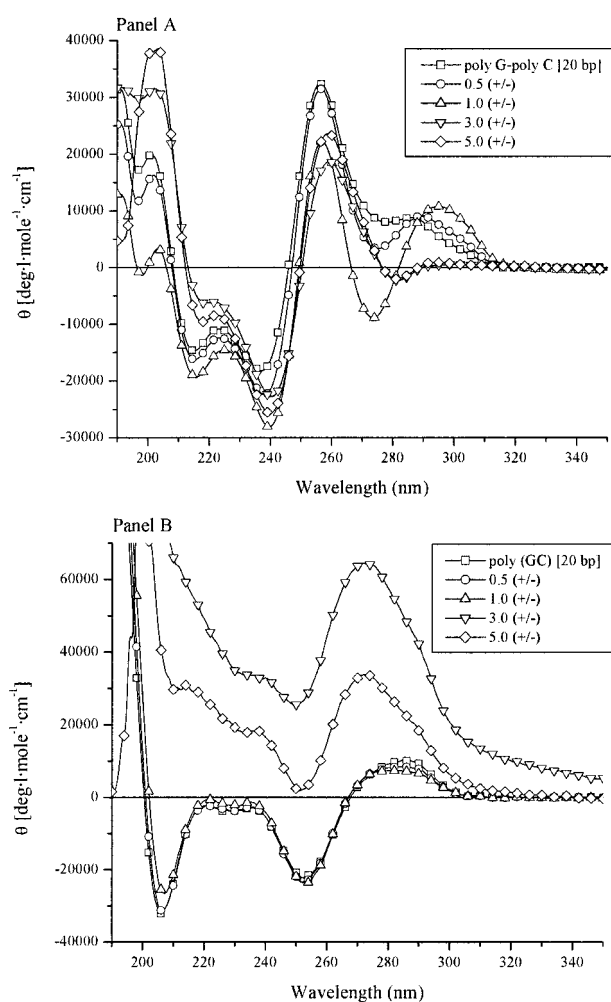

FIGURE 5 Representative CD spectra of 20 bp ODN complexes, DOTAP/poly(dG) · poly(dC) (*A*) and DOTAP/poly(dGdC) · poly(dGdC) (*B*). The charge ratio is indicated in the legend. Oligonucleotide (100 μg/ml), open squares; 0.5 charge ratio, open circles; 1.0 charge ratio, open triangles; 3.0 charge ratio, open inverted triangles; 5.0 charge ratio, open diamond. In (*B*), spectra at 3.0 and 5.0 charge ratios are indicative of PSI-type spectra.

DISCUSSION

The conformational state of DNA in CLDCs is contentious. CD studies suggest cationic lipids induce a B→C change in secondary structure (Akao et al., 1996; Zuidam et al., 1999;

TABLE 1   DOTAP/Oligonucleotide CD spectral peak values

Lipid composition		245 nm				275 nm			
		Peak position*	A	B	C	Peak position*	A	B	C
poly(G)·poly(C) 4 kbp	% Diff. (+/−)	235.5 nm	152% (1.0)	178% (4.0)	171% (5.0)	282.4 nm	21% (1.0)	−4% (4.0)	0% (5.0)
poly(G)·poly(C) 20 bp	% Diff. (+/−)	237.0 nm	154% (1.0)	125% (3.0)	141% (5.0)	278.1 nm	−11% (1.0)	−29% (3.0)	−25% (5.0)
poly(A)·poly(T) ~229 bp	% Diff. (+/−)	247.3 nm	92% (1.0)	94% (3.0)	117% (5.0)	259.1 nm	91% (1.0)	93% (3.0)	122% (5.0)
poly(A)·poly(T) 20 bp	% Diff. (+/−)	248.0 nm	106% (1.0)	28% (3.0)	51% (5.0)	260.2 nm	71% (1.0)	221% (3.0)	197% (5.0)
poly(GC)·poly(GC) 724 bp	% Diff. (+/−)	251.5 nm	127% (1.0)	130% (3.0)	127% (5.0)	273.7 nm	85% (1.0)	62% (3.0)	78% (5.0)
poly(GC)·poly(GC) 20 bp	% Diff. (+/−)	252.7 nm	106% (1.0)	−83% (3.0)	−10% (5.0)	285.6 nm	75% (1.0)	560% (3.0)	328% (5.0)
poly(AT)·poly(AT) 3.2 kbp	% Diff. (+/−)	246.9 nm	108% (1.0)	114% (4.0)	114% (5.0)	262.5 nm	55% (1.0)	52% (3.0)	58% (5.0)
poly(AT)·poly(AT) 20 bp	% Diff. (+/−)	247.5 nm	87% (1.0)	−34% (4.0)	−27% (5.0)	267.6 nm	108% (1.0)	462% (4.0)	431% (5.0)

*Position of peak maximum (± 0.3 nm)
(*A*) Change in peak intensity at peak maximum at a CLDC charge ratio of 1:1.
(*B*) Change in peak intensity at peak maximum at the charge ratio where maximum change occurs. The value of this charge ratio is given in parentheses.
(*C*) Change in peak intensity at peak maximum at the high CLDC charge ratio of 5:1.

Patil and Rhodes, 2000; Zhang et al., 2002). This is based on the observation that increasing cationic lipid concentrations cause the long wavelength (~275 nm) peak to decrease in height whereas the negative band (~245 nm) maintains its intensity. Although a loss of 275 nm CD intensity compared to that of B form is, in fact, characteristic of C form, a 245-nm band intensity approximately two-thirds that of the B form is thought to be more characteristic of the C state (Bokma et al., 1987). The reduced 275-nm band and intensification of the 245-nm band we observe, however, more closely resemble cation-induced spectral changes that have been attributed to a noncooperative increase in DNA winding angle (from 10.4→10.2 bp/turn) that maintains the B form geometry (Bokma et al., 1987). In the latter case, a collapse of the 275-nm peak with little alteration of the 245-nm band is seen (Bokma et al., 1987; Bloomfield et al., 1999). It is clear from our studies that although dispersive light scattering perturbs band intensities, neither absorption flattening nor differential scattering is sufficient to account for these changes.

FTIR suggests that the sugar-base conformation of the plasmid in CLDCs maintains the C2′-endo-anti geometry. This nucleotide conformation excludes many secondary structures, but the B and C forms share this arrangement. Both are members of a class of structural states that have two nucleotide conformations (B_I and B_{II}), which differ in their phosphate orientations (van Dam and Levitt, 2000). C form is generally considered to arise when the B_{II} geometry makes up ≥45% of the nucleotide population (van Dam and Levitt, 2000). The change from B to C forms is therefore non-cooperative, unlike most ODN conformational changes. Nevertheless, IR spectra are still capable of distinguishing the two forms inasmuch as many vibrational states undergo changes in B→C transformations. Signals from the G/T carbonyl, phosphodiester and asymmetric phosphate vibrations reportedly shift to 1710, 960, and 1231 cm^{-1}, respectively, in C form (Adam et al., 1987; Taillandier and Liquier, 1992; Pichler et al., 1999; Loprete and Hartman, 1989). In this work, the 970 cm^{-1} band is unchanged,
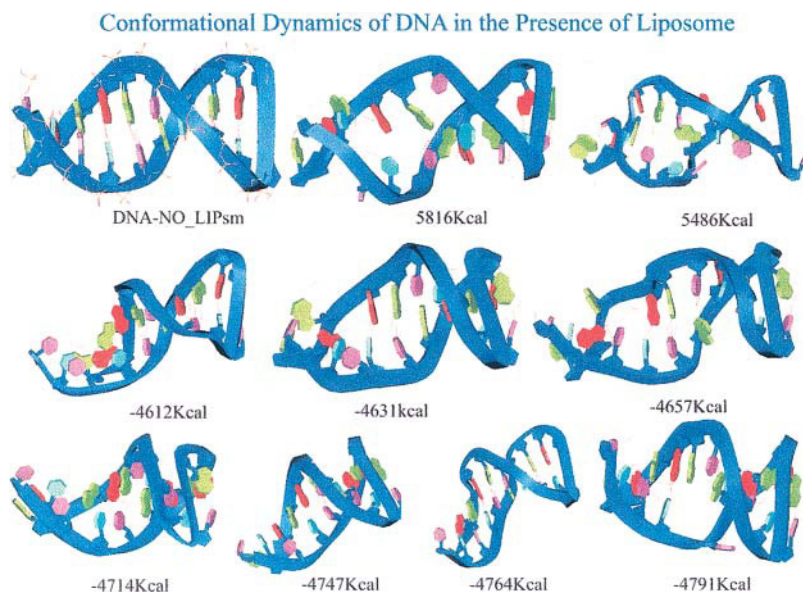

FIGURE 6   Images of the DNA conformation at selected time points in the dynamic simulation of dsDNA (CTCTCGAGAG) interacting with 1,2-dimyristoyl-*sn*-glycero-3-phosphocholine. The images are arranged in order of increasing favorable free energy with the free energy of each state given below each image.

whereas the 1715 cm^{-1} and 1223 cm^{-1} shift but to frequencies inconsistent with C form. The relative intensity of the symmetric phosphate vibration either weakly (1089 cm^{-1}) or strongly (1109 cm^{-1}) hydrogen-bonded has been shown to correlate with the B$_I$ and B$_{II}$ conformations, respectively (Pichler et al., 1999). Although an increase in the 1109 cm^{-1} intensity is apparent in Raman CLDC spectra, this is probably due to electrostatic interactions between the lipid and DNA phosphate, because the 1109 cm^{-1} band is absent in FTIR spectra. This suggests that B$_I$ nucleotides remain the predominant conformation in DNA complexed with cationic lipid. One cannot exclude some change in the relative distribution of the B$_I$ and B$_{II}$ forms, however.

Recently a deoxyoligonucleotide duplex (CCCCGGGG) exhibiting an intermediate B/A conformation has been described (Trantirek et al., 2000). The conformation of this duplex has a B-type sugar phosphate backbone (deoxyribose sugar pucker). The bases, however, are shifted from the helix center to the periphery with a wide minor groove appearing at the midpoint of the ODN, an arrangement characteristic of the A form. This intermediate state results from the tendency of guanosine-guanosine stacking to adopt an A-like conformation even within an overall B-DNA helix (Stefl et al., 2001). This polymorphism of local base stacking interactions while maintaining a B-form backbone geometry is consistent with the altered CD spectra occurring in CLDCs and the diverse structures seen at longer times in the molecular dynamics generated images (Fig. 6).

An alternative hypothesis to explain the large changes induced in the CD spectrum of DNA by cationic lipids involves the formation of some type of supramolecular structure whose spectral contribution subtracts from the native DNA spectrum (Zuidam et al., 1999). Such structure is usually thought to arise from long-range interactions primarily within DNA molecules but not necessarily in a condensed state. Studies of linear ODNs ranging from 20 bp to 4000 basepairs, however, show no obvious correlation between basepair length and the spectral intensities of the DNA within CLDCs. This suggests that the CD spectra of cationic lipid/DNA complexes cannot be directly explained by the presence of such structures.

Some hints about the origin of the altered nature of the DNA spectra may be obtained from FTIR and Raman spectroscopies, which provide evidence of altered hydrogen bonding in the bases. Shifts in the FTIR vibrations of the guanine carbonyl and imidazole nitrogen (N7) upon complexation have both been interpreted as reflecting altered hydrogen bonding (Choosakoonkriang et al., 2001a). In Raman spectra, a similar response in the guanine imidazole nitrogen is observed upon complexation. The guanine N7 (1488 cm^{-1}) disappears, whereas a prominent peak at 1465 cm^{-1}, indicative of the hydrogen bonded state, appears (Peticolas et al., 1987). The reduced intensity of the adenine exocyclic amine N6 (1422 cm^{-1}) and ring N3 (1578 cm^{-1})

observed in complexes has been associated with hydrogen bonding (Peticolas et al., 1987). These sites on purine nucleotides are each accessible from the major groove except for the adenine/guanine ring N3, which can be contacted through the minor groove.

Studies of the binding of a cationic amine to DNA produce CD spectra similar to those induced by CLDCs (Chen et al., 1981). In these investigations, calf thymus DNA was modified by covalent binding of butyl amine (BuA) to minor groove guanine exocyclic amines (Chen et al., 1981; Maibenco et al., 1989). Attachment at 12–15% of the bases produced CD spectra with loss of ~90% of the 275-nm peak intensity with little change in 245-nm band values (Chen et al., 1981). These CD spectral changes were interpreted in terms of the presence of a variant B form with increased winding angle (Fish et al., 1983; Chen et al., 1983). Interestingly, titration of the adducts' ionization state demonstrates reversibility of the 275-nm intensity change, implying that the charged state of the BuA is critical. Another alternative suggested by the authors is that direct perturbation of the bases by the positively charged bound amine may be involved in the CD spectral changes. The presence of the positively charged headgroup in the cationic lipids studied here could play a corresponding role. Whatever explanation is correct, a significant disruption of the planar interaction between the bases would seem to provide the most direct explanation for the decrease in rotational strength seen here.

Although lack of structural parameters for a suitable cationic lipid prevented building an ideal model, we used a positively charged form of DMPC to mimic a cationic lipid surface and performed a molecular dynamics study of the interaction of this lipid with a 10-bp duplex of DNA. Striking alterations in DNA structure were observed in this model of DNA/lipid interaction. The changes in helicity and base stacking clearly observed in Fig. 6 are undoubtedly excessive due to lack of hydration and the potential conformational mobility of the DNA and DMPC components, which would be expected to be reduced by the DNAs sandwiching between lipid bilayers in actual CLDCs. Nevertheless, it seems clear that lipid/DNA interactions extend beyond direct electrostatic coupling between the lipid headgroup and phosphate backbone to interactions between headgroups and DNA bases. This, in turn, produces alterations in base stacking interactions that would be expected to reduce the intensity of CD signals arising from electrostatic and magnetic coupling between bases. The BuA adduct model demonstrates that a small number of modified sites can have a large effect on CD spectra, implying that limited structural changes could be responsible for the large CD changes seen upon cationic lipid and DNA interaction. In the case of actual plasmid complexes, it seems that disruptive interactions could be limited by both accessibility and competing torsional forces in the supercoiled DNA.

G.S.J. thanks Prof. Krzysztof Kuezera for granting access to computational facilities.

REFERENCES

Adam, S., P. Bourtayre, J. Liquier, J. A. Taboury, and E. Taillandier. 1987. Poly[d(A-T)-Cs+] conformations studied by IR spectroscopy. *Biopolymers*. 26:251–260.

Akao, T., T. Fukumoto, H. Ihara, and A. Ito. 1996. Conformational change in DNA induced by cationic bilayer membranes. *FEBS Lett*. 391:215–218.

Bloomfield, V. A., D. M. Crothers, and I. Tinoco Jr. 1999. Nucleic Acids: Structures, Properties, and Functions. University Science Books, Sausalito, CA.

Bokma, J. T., W. C. J. Johnson, and J. Blok. 1987. CD of Li-salt of DNA in ethanol/water mixtures: evidence for the B- to C- form transition in solution. *Biopolymers*. 26:893–909.

Braun, C. S., L. A. Kueltzo, and C. R. Middaugh. 2001. Ultraviolet absorption and circular dichroism spectroscopy of nonviral gene delivery complexes. *In* Methods in Molecular Medicine: Nonviral Vectors for Gene Therapy. M. A. Findeis, editor. Humana Press, Totowa, NJ. 253–284.

Brooks, B. R., R. Bruccoleri, B. Olafson, D. States, S. Swaminathan, and M. Karplus. 1983. CHARMM: a program for macromolecular energy, minimization and dynamics calculations. *J Comp Chem*. 4:187–217.

Bustamante, C., I. Tinoco Jr., and M. F. Maestre. 1983. Circular differential scattering can be an important part of the circular dichroism of macromolecules. *Proc. Natl. Acad. Sci. USA*. 80:3568–3572.

Chen, C., R. Kilkuskie, and S. Hanlon. 1981. Circular dichroism spectral properties of covalent complexes of deoxyribonucleic acid and n-butylamine. *Biochemistry*. 20:4987–4995.

Chen, C. Y., B. H. Pheiffer, S. B. Zimmerman, and S. Hanlon. 1983. Conformational characteristics of deoxyribonucleic acid-butylamine complexes with C-type circular dichroism spectra. 1. An X-ray fiber diffraction study. *Biochemistry*. 22:4746–4751.

Choosakoonkriang, S., C. M. Wiethoff, T. J. Anchordoquy, G. S. Koe, J. G. Smith, and C. R. Middaugh. 2001a. Infrared spectroscopic characterization of the interaction of cationic lipids with plasmid DNA. *J. Biol. Chem*. 276:8037–8043.

Choosakoonkriang, S., C. M. Wiethoff, L. A. Kueltzo, and C. R. Middaugh. 2001b. Characterization of synthetic gene delivery vectors by infrared spectroscopy. *In* Methods in Molecular Medicine: Nonviral Vectors for Gene Therapy. M. A. Findeis, editor. Humana Press, Totowa, NJ. 285–317.

Colthup, N. B., L. H. Daly, and S. E. Wiberley. 1975. Introduction to Infrared and Raman Spectroscopy. Academic Press, New York.

Davies, M. A., H. F. Schuster, J. W. Brauner, and R. Mendelsohn. 1990. Effects of cholesterol on conformational disorder in dipalmitoylphosphatidylcholine bilayers. A quantitative IR study of the depth dependence. *Biochemistry*. 29:4368–4373.

Deng, H., V. A. Bloomfield, J. M. Benevides, and G. J. Thomas, Jr. 2000. Structural basis of polyamine-DNA recognition: spermidine and spermine interactions with genomic B-DNAs of different GC content probed by Raman spectroscopy. *Nucleic Acids Res*. 28:3379–3385.

Erfurth, S. C., E. J. Kiser, and W. L. Peticolas. 1972. Determination of the backbone structure of nucleic acids and nucleic acid oligomers by laser Raman scattering. *Proc. Natl. Acad. Sci. USA*. 69:938–941.

Felgner, J. H., R. Kumar, C. N. Sridhar, C. J. Wheeler, Y. J. Tsai, R. Border, P. Ramsey, M. Martin, and P. L. Felgner. 1994. Enhanced gene delivery and mechanism studies with a novel series of cationic lipid formulations. *J. Biol. Chem*. 269:2550–2561.

Feller, S. E., and R. W. Pastor. 1999. Constant surface tension simulations of lipid bilayers: the sensitivity of surface areas and compressivities. *J. Chem. Phys*. 111:1281–1287.

Fish, S. R., C. Y. Chen, G. J. Thomas Jr., and S. Hanlon. 1983. Conformational characteristics of deoxyribonucleic acid-butylamine complexes with C-type circular dichroism spectra. 2. A Raman spectroscopic study. *Biochemistry*. 22:4751–4756.

Foloppe, N., and A. D. MacKerell. 1998. Conformational properties of the deoxyribose and ribose moieties of nucleic acids: a quantum mechanical study. *J. Phys. Chem*. 102:6669–6678.

Foloppe, N., and A. D. MacKerell. 1999. Intrinsic conformational properties of deoxyribonucleosides: implicated role for cytosine in the equilibrium among the A, B, and Z forms of DNA. *Biophys. J*. 76:3206–3218.

Glaeser, R. M., and B. K. Jap. 1985. Absorption flattening in the circular dichroism spectra of small membrane fragments. *Biochemistry*. 24:6398–6401.

Goodsell, D. S., K. Grzeskowiak, and R. E. Dickerson. 1995. Crystal structure of C-T-C-T-C-G-A-G-A-G. Implications for the structure of the Holliday junction. *Biochemistry*. 34:1022–1029.

Hafez, I. M., N. Maurer, and P. R. Cullis. 2001. On the mechanism whereby cationic lipids promote intracellular delivery of polynucleic acids. *Gene Ther*. 8:1188–1196.

Hirsch-Lerner, D., and Y. Barenholz. 1999. Hydration of lipoplexes commonly used in gene delivery: follow-up by laurdan fluorescence changes and quantification by differential scanning calorimetry. *Biochim Biophys Acta*. 1461:47–57.

Huang, L., M. C. Hung, and E. Wagner. 1999. Non-Viral Vectors for Gene Therapy. Academic Press, San Diego.

Ivanov, V. I., L. E. Minchenkova, A. K. Schyolkina, and A. I. Poletayev. 1973. Different conformations of double-stranded nucleic acid in solution as revealed by circular dichroism. *Biopolymers*. 12:89–110.

Johnson, W. C. 1994. CD of nucleic acids. *In* Circular Dichroism: Principles and Applications. K. Nakanishi, N. Berova, and R. W. Woody, editors. VCH Publishers, New York. 523–540.

Johnson, W. C. 1996. Determination of the conformation of nucleic acids by electronic CD. *In* Circular Dichroism and the Conformational Analysis of Biomolecules. G. D. Fasman, editor. Plenum Press, New York. 433–468.

Kabanov, A. V., P. L. Felgner, and L. W. Seymour. 1998. Self-Assembling Complexes for Gene Delivery: From Laboratory to Clinical Trial. John Wiley & Sons, New York.

Keller, D., and C. Bustamante. 1986a. Theory of the interaction of light with large inhomogeneous molecular aggregates. I. Absorption. *J. Chem. Phys*. 84:2961–2971.

Keller, D., and C. Bustamante. 1986b. Theory of the interaction of light with large inhomogeneous molecular aggregates. II. Psi-type circular dichroism. *J. Chem. Phys*. 84:2972–2980.

Koltover, I., T. Salditt, J. O. Rädler, and C. R. Safinya.1998. An inverted hexagonal phase of cationic liposome-DNA complexes related to DNA release and delivery. *Science*. 281:78–81.

Koppel, D. E. 1972. Analysis of macromolecular polydispersity in intensity correlation spectroscopy: the method of cumulants. *J. Chem. Phys*. 57:4814–4820.

Loprete, D. M., and K. A. Hartman. 1989. Existence of the C structure in poly(dA-dC)-poly(dG-dT). *J. Biomol. Struct. Dyn*. 7:347–362.

Maestre, M. F., and C. Reich. 1980. Contribution of light scattering to the circular dichroism of deoxyribonucleic acid films, deoxyribonucleic acid-polylysine complexes, and deoxyribonucleic acid particles in ethanolic buffers. *Biochemistry*. 19:5214–5223.

Maibenco, D., P. Tang, R. Shinn, and S. Hanlon. 1989. Base and conformational specificity of an amine modification of DNA. *Biopolymers*. 28:549–571.

Mao, D., and B. A. Wallace. 1984. Differential light scattering and absorption flattening optical effects are minimal in the circular dichroism spectra of small unilamellar vesicles. *Biochemistry*. 23:2667–2673.

Mendelsohn, R., M. A. Davies, J. W. Brauner, H. F. Schuster, and R. A. Dluhy. 1989. Quantitative determination of conformational disorder in the acyl chains of phospholipid bilayers by infrared spectroscopy. *Biochemistry*. 28:8934–8939.

Mendelsohn, R., M. A. Davies, H. F. Schuster, Z. C. Xu, and R. Bittman. 1991. CD2 rocking modes as quantitative infrared probes of one-,

two-, and three-bond conformational disorder in dipalmitoylphosphatidyl-choline and dipalmitoylphosphatidylcholine/cholesterol mixtures. *Biochemistry*. 30:8558–8563.

Nishimura, Y., and M. Tsuboi. 1986. Local conformations and polymorphism of DNA duplexes as revealed by their Raman spectra. *Adv. Spectrosc.* 13:177–232.

Patil, S. D., and D. G. Rhodes. 2000. Conformation of oligodeoxynucleotides associated with anionic liposomes. *Nucleic Acids Res.* 28:4125–4129.

Peticolas, W. L., and E. Evertsz. 1992. Conformation of DNA in vitro and in vivo from laser Raman scattering. *Methods Enzymol.* 211:335–352.

Peticolas, W. L., W. L. Kubasek, G. A. Thomas, and M. Tsuboi. 1987. Nucleic acids. *In* Biological Applications of Raman Spectroscopy. T. G. Spiro, editor. John Wiley & Sons, New York. 81–133.

Pichler, A., S. Rudisser, M. Mitterbock, C. G. Huber, R. H. Winger, K. R. Liedl, A. Hallbrucker, and E. Mayer. 1999. Unexpected BII conformer substate population in unoriented hydrated films of the d(CGCGAATTCGCG)2 dodecamer and of native B-DNA from salmon testes. *Biophys. J.* 77:398–409.

Radler, J. O., I. Koltover, A. Jamieson, T. Salditt, and C. R. Safinya. 1998. Structure and interfacial aspects of self-assembled cationic lipid-DNA gene carrier complexes. *Langmuir.* 14:4272–4283.

Rodger, A., and M. A. Ismail. 2000. Spectrophotometry and Spectrofluorimetry. Oxford University Press, New York.

Schlenkrich, M., J. Brickmann, A. D. MacKerell, and M. Karplus. 1996. Empirical Potential Energy Function for Phospholipids: Criteria for Parameter Optimization and Applications. Birkhauser, Boston.

Serban, D., J. M. Benevides, and G. J. Thomas Jr. 2002. DNA secondary structure and Raman markers of supercoiling in Escherichia coli plasmid pUC19. *Biochemistry.* 41:847–853.

Simberg, D., D. Danino, Y. Talmon, A. Minsky, M. E. Ferrari, C. J. Wheeler, and Y. Barenholz. 2001. Phase behavior, DNA ordering, and size instability of cationic lipoplexes. Relevance to optimal transfection activity. *J. Biol. Chem.* 276:47453–47459.

Stefl, R., L. Trantirek, M. Vorlickova, J. Koca, V. Sklenar, and J. Kypr. 2001. A-like guanine-guanine stacking in the aqueous DNA duplex of d(GGGGCCCC). *J. Mol. Biol.* 307:513–524.

Taillandier, E., and J. Liquier. 1992. Infrared spectroscopy of DNA. *Methods Enzymol.* 211:307–335.

Thomas, G. A., and W. L. Peticolas. 1983a. Flexibility of nucleic acid conformations. 1. Comparison of the intensities of the Raman-active backbone vibrations in double-helical nucleic acids and model double-helical dinucleotide crystals. *J. Am. Chem. Soc.* 105:986–992.

Thomas, G. A., and W. L. Peticolas. 1983b. Fluctuations in nucleic acid conformations. 2. Raman spectroscopic evidence of varying ring pucker in A-T polynucleotides. *J. Am. Chem. Soc.* 105:993–996.

Tinoco, I., C. Bustamante, and M. Maestre. 1980. The optical activity of nucleic acids and their aggregates. *Annu. Rev. Biophys. Bioeng.* 9:107–141.

Trantirek, L., R. Stefl, M. Vorlickova, J. Koca, V. Sklenar, and J. Kypr. 2000. An A-type double helix of DNA having B-type puckering of the deoxyribose rings. *J. Mol. Biol.* 297:907–922.

van Dam, L., and M. H. Levitt. 2000. BII nucleotides in the B and C forms of natural-sequence polymeric DNA: A new model for the C form of DNA. *J. Mol. Biol.* 304:541–561.

Wallace, B. A., and C. L. Teeters. 1987. Differential absorption flattening optical effects are significant in the circular dichroism spectra of large membrane fragments. *Biochemistry.* 26:65–70.

Xu, Y., S. W. Hui, P. Frederik, and F. C. Szoka. 1999. Physicochemical characterization and purification of cationic lipoplexes. *Biophys. J.* 77:341–353.

Zhang, Z., W. Huang, J. Tang, E. Wang, and S. Dong. 2002. Conformational transition of DNA induced by cationic lipid vesicle in acidic solution: spectroscopy investigation. *Biophys. Chem.* 97:7–16.

Zuidam, N., Y. Barenholz, and A. Minsky. 1999. Chiral DNA packaging in DNA-cationic liposome assemblies. *FEBS Lett.* 457:419–422.